Article

pubs.acs.org/Biomac

Facile Route to Produce Chitin Nanofibers as Precursors for Flexible and Transparent Gas Barrier Materials

Jie Wu,[†] Kuang Zhang,[‡] Natalie Girouard,[‡] and J. Carson Meredith*[,‡]

[†]School of Materials Science and Engineering and [‡]School of Chemical and Biomolecular Engineering, Georgia Institute of Technology, Atlanta, Georgia 30332, United States

ABSTRACT: Chitin is the second most abundant biopolymer in nature and has tremendous potential in renewable materials for packaging, energy storage, reinforced composites, and biomedical engineering. Despite attractive properties, including biodegradability, antibacterial activity, and high strength, chitin is not utilized widely due to strong molecular interactions, which make solubilization and processing difficult. We report a high pressure homogenization route to produce pure chitin nanofibers (ChNFs) starting with a mildly acidic aqueous dispersion of purified crab α-chitin. The well-dispersed ChNFs with diameter ~20 nm do not form strong network structures under conditions explored herein and can be directly processed into useful materials, bypassing the need to dissolve the chitin. Dried ChNFs form pure self-standing chitin films with the lowest to-date reported O_2 and CO_2 permeabilities of 0.006 and 0.018 barrer, respectively. Combined with high flexibility and optical transparency, these materials are ideal candidates for sustainable barrier packaging.

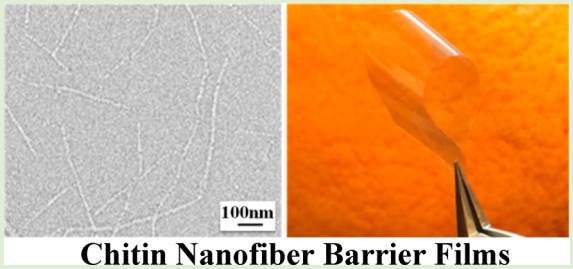

INTRODUCTION

Developing renewable materials to reduce the dependence on fossil fuel as a feedstock for a wide range of applications is becoming increasingly important to society.[1,2] Chitin, poly(β-(1−4)-*N*-acetyl-D-glucosamine), is the second most abundant biopolymer with 10^{10} to 10^{11} tons produced annually in nature. Due to strong hydrogen bonding, chitin occurs as highly crystalline nanofibers (ChNFs) that assemble into hierarchical structures. Chitin is renewable, biodegradable, and antibacterial and its crystallinity leads to high stiffness, strength, and barrier properties, supporting applications in barrier packaging. However, chitin crystallinity creates extraction and processing challenges.[3−7]

Two main approaches have been utilized to process native chitin: (1) regeneration, where the chitin is dissolved and then precipitated, or (2) extraction/dispersion, in which chitin micro- or nanofibers are recovered from native chitin as a dispersion. Regeneration approaches include production of chitin-based nanofibers from dissolved chitin by electrospinning, phase separation, and coagulant-induced gelation of solutions.[8−10] These techniques rely on the utilization of strong acids, bases or volatile organic solvents that detract from chitin's sustainability and disrupt its intrinsically high crystallinity. An alternative is top-down production of dispersed ChNF building blocks that can be controllably assembled into useful materials without requiring solubilization. For example, ChNFs were extracted from crab shell α-chitin and squid pen β-chitin using mechanical grinding and high-power ultrasonication, respectively,[11−13] which formed a highly viscous gel,[11−13] which supports film formation but also can create processing challenges.[14] Ultrasonication was not able to disintegrate ChNFs from crab α-chitin, possibly due to the higher crystallinity, antiparallel configuration and greater intermolecular interactions of α-chitin compared with β-chitin.[11]

Currently, there is great demand for bioderived gas barrier materials for food, beverage and medical packaging and polysaccharides are of interest because of their reduced environment impact relative to conventional plastics.[10,15−17] Cellulose has been utilized for many decades as a barrier in "cellophane", and recent studies report that micro- or nanofibrillated cellulose films show promise as barrier films.[16] Films with oxygen barrier properties that meet or exceed those of commercial barrier polymers (poly(ethylene terephthalate) (PET), poly(vinyl chloride), and poly(vinylidene chloride)) have been reported for nanofibrillated cellulose from high-pressure fluidization,[18] TEMPO-oxidized cellulose nanowhiskers,[19] and cellulose coagulated from NaOH/urea/water solution.[20] Few reports of chitin barrier properties have been published, and in contrast to cellulose, self-standing pure chitin films with high barrier properties have not been reported. Regenerated chitin films plasticized with glycerol, produced from NaOH/urea/water solutions, had an impressive O_2 permeability of 0.003 barrer (35 °C).[10] Composite films of TEMPO-oxidized chitin nanowhiskers coated on PLA are reported to have an O_2 permeability of 0.001 barrer.[21] An important advance would be the ability to produce self-standing, pure chitin films with combined transparency, flexibility, and barrier properties, by using an aqueous

Received: September 22, 2014
Revised: November 6, 2014
Published: November 19, 2014

   dx.doi.org/10.1021/bm501416q | *Biomacromolecules* 2014, 15, 4614−4620

fibrillation and casting process that does not require dissolution of chitin. This goal is the focus of the present study.

In this study, starting from crab α-chitin powder, we report a high-pressure homogenization method that produces water-dispersed ChNFs with narrow diameter distribution and rheological properties suitable for facile processing. Self-standing, pure chitin films prepared from these ChNF dispersions are transparent, mechanically robust, and flexible, and have gas barrier properties for O_2 and CO_2 that meet or exceed those of the conventional petroleum-based barrier polymers like PET.

EXPERIMENTAL SECTION

Materials. Dried crab shell flakes were purchased from TCI America. Deionized water (18.2 MΩ cm) was prepared in a Barnstead Easypure RoDi purification system. Hydrochloric acid, sodium hydroxide, acetone and ethanol were purchased from EMD Chemical Inc.

Methods. Dried crab shell flakes were processed to obtain purified chitin using a method developed from previous literature.[3,12,14] Ground crab shells were refluxed in 5 wt % sodium hydroxide in DI water for 6 h. The suspension was filtered and washed with DI water until the pH was 7. Subsequently, the filtered solids were treated with 7% hydrochloric acid for 6 h at room temperature. After filtration and washing with DI water, the treated sample was refluxed in a 5% NaOH solution for 2 days to remove residual proteins and the other residues were eliminated by acetone and ethanol extraction. The purified chitin was dispersed in DI water under acidic condition (aqueous pH ∼ 4) by magnetic stirring, where HCl was used to adjust medium pH. To generate ChNFs, this mixture was processed through a high-pressure homogenizer by using a 0.20 mm nozzle (Bee International Inc., MA) operating at a pressure of 15000 psi and room temperature for 20 passes, followed by homogenization with a 0.13 mm nozzle operating at a pressure of 22,000 psi and room temperature for 10 passes. The resulting ChNF/water dispersion was cast into a Petri dish, followed by drying at room temperature for 6 days to produce solid ChNF films.

The degree of acetylation (DA) of the purified chitin was characterized using ^{13}C cross-polarization under magic-angle spinning (CP-MAS) NMR, which was performed on a Bruker 400 spectrometer with a spinning rate of 5 kHz, contact times of 1 ms, and pulse intervals of 5 s.[22] The DA of chitin was determined using the ratio of the integral of methyl carbon atom of the N-acetyl group to the summation integrals of the six carbon atoms of the D-glucopyranosyl ring (C_1−C_6 atoms: δ 50 to 105 ppm)[23]

$$\mathrm{DA} = 100 \times (I_{\mathrm{N-CH_3}})/\left(\frac{1}{6}\sum I_{\text{main chain carbons}}\right) \quad (1)$$

The light transmittances (wavelengths: 400−800 nm) of chitin dispersions and ChNF solid films were measured using a UV−vis spectrometer (JASCO-V630). A cuvette filled with DI water was used as a reference for chitin dispersion measurement. The morphologies of chitin-based materials were obtained using field emission scanning electron microscopy (Zeiss Ultra 60). Before imaging, these samples were coated with a thin layer of gold/palladium (Hummer IV Sputtering System) to promote conductivity. The surface features of ChNF film were characterized using atomic force microscopy (AFM, Veeco Dimension 3100). The flat film was first attached onto a smooth silicon wafer, and then the images were collected under tapping mode. The cantilever had a nominal spring constant of 37 N/m and a nominal frequency of 300 kHz (Applied NanoStructures, Inc., Santa Clara, CA). The surface charge of ChNFs at pH 4.1 in water was measured by a Malvern Zetasizer Nano ZS 90.

Dynamic rheology of ChNF dispersions (0.5 wt % of chitin) was carried out by a MCR 300 rheometer (Anton Paar, Graz, Austria) using a plate and plate geometry at 23 °C. Before the dynamic viscoelastic measurements, the linear viscoelastic region was accessed by a strain sweep experiment in the range of 0.01 to 10% at a frequency of 1 Hz. The frequency sweep was conducted from 0.1 to 10 rad/s with a controlled stain of 0.005, which was within the linear viscoelastic region. Shear viscosity was measured by increasing the shear rate from 0.1 to 1001/s at 23 °C. The attenuated total reflectance-Fourier transform infrared spectra (ATR-FTIR) of chitin powders and ChNF films were recorded using Bruker platinum ATR connected to a Bruker Vertex 80 FTIR (Bruker Optics, Inc., Billerica, MA).

Water absorption in ChNF films was assessed with thermogravimetric analysis (TGA, TA Instruments TGA Q50). Approximately 5−10 mg of sample was loaded into the ceramic pan. The sample was heated from room temperature to 120 °C at a rate of 10 °C/min under a flowing nitrogen atmosphere (N_2 purity > 99.999%, gas flow rate: 50 mL/min) and then held at 120 °C for 30 min. The amount of water absorbed was calculated by the mass loss during these two steps. Density of the ChNF films was determined at 23 °C using a density gradient column containing calcium nitrate-water solution (Techne, Burlington, NJ). To limit the effect of water uptake on sample density, the density measurements were recorded 20 min after introducing the samples into the column. The porosities of ChNF films were determined using eq 2. The density of chitin is taken to be 1425 kg/m^3.[14]

$$\text{porosity} = 1 - \frac{\rho_{\text{ChNF film}}}{\rho_{\text{chitin}}} \quad (2)$$

The ultimate tensile strength, Young's modulus and ultimate strain at break of ChNF films were measured using a RSA III Dynamic Mechanical Analyzer (TA Instruments) at room temperature. At least 3 specimens with dimensions of 50 mm in length, 3 mm in width, and 30 μm in thickness were cut from the films and were tested at a strain rate of 0.6 mm/min with a gap distance of 10 mm. Uniaxial tensile testing was also performed using a Universal Testing Machine (MTS Systems, Insight 2) equipped with a 100 N load cell, by using samples cut into strips measuring approximately 35 mm in length and 3 mm in width. The test section measured 13 mm and the strain rate was 1.3 mm/min. The strain rate and sample width were chosen based on ASTM D882−10. All samples were 0.03 mm thick. The grips were lined with crocus cloth in order to mitigate slipping.

Gas permeabilities of ChNF films were measured using a constant volume permeation system at room temperature and 0% relative humidity. The detailed experimental setup has been described previously.[24] Briefly, a ChNF film was first sandwiched between two concentric pieces of impermeable aluminum tape and then was assembled into a permeation cell. The cell was subsequently loaded in the permeation system. The entire permeation system was degassed for over 24 h. After a leak test, the upstream was pressurized with feed gas (O_2, N_2, H_2, CO_2, or CH_4), while the downstream was kept at vacuum. The pressure change in a constant downstream volume was recorded over time and the permeability of ChNF film was calculated based on eq 3,

$$P = \frac{(2.94 \times 10^4)(VL)(dp/dt)}{TA\Delta p} \quad (3)$$

where V is the downstream volume, L is the thickness of measured film, dp/dt is the steady state rate of pressure rise, T is the absolute temperature, A is the measured film area, and Δp is the pressure difference between the upstream and downstream.[24]

RESULTS AND DISCUSSION

Crab shells mainly consist of proteins, minerals and chitin.[5−7] To obtain the purified chitin starting material, a series of chemical treatments were performed on crab shells, including acid treatment to remove minerals and base treatment to deplete proteins. The degree of acetylation (DA) is an important parameter of chitin and has been used to differentiate chitin from chitosan. While all natural chitin contains some substitution with chitosan along the chain, the polymer is called

chitin when DA is greater than 50%.[6,7] Here, a nondestructive method, ^{13}C CP-MAS solid state NMR, was used to determine the DA of the purified chitin from crab shells. The positions of C_1, C_2, C_3, C_4, C_5, C_6, and $N-CH_3$ in ^{13}C NMR spectra are 104.36, 55.54, 73.81, 83.51, 75.91, 61.20, and 23.17 ppm, as illustrated in Figure 1. According to eq 1, the DA of purified chitin is 92.4%.

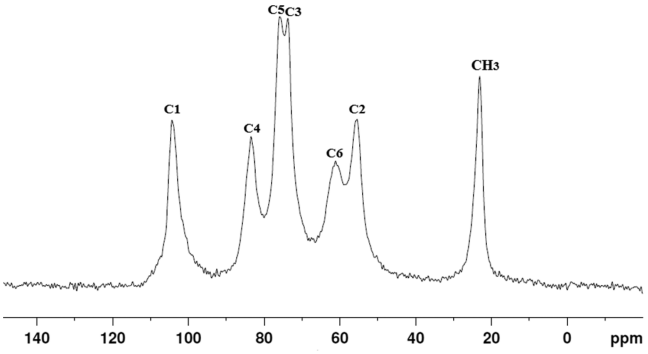

Figure 1. ^{13}C CP-MAS solid state NMR of purified chitin from crab shells.

Crab shells have intricate hierarchical structures that are mainly produced by the assembly of chitin and proteins, and ChNFs are its key elements.[5] The purified chitin was obtained as micron-sized particles, and it consisted of fibers with diameters ranging from a few tens of nanometers to hundreds of nanometers (Figure 2A,B). When the purified chitin/water

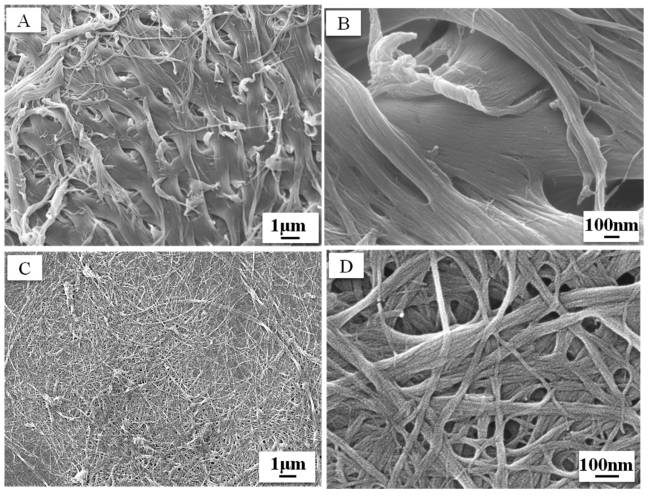

Figure 2. (A, C) SEM images of the purified chitin and chitin that was produced by a high pressure homogenization process of a neutral chitin/water dispersion (pH 7), respectively. (B, D) SEM images with higher magnification in comparison to (A) and (C), respectively.

dispersion with a neutral pH of 7 was treated by a high pressure homogenization process that includes 20 passes with a 0.20 mm nozzle at 15000 psi and 15 passes with a 0.13 mm nozzle at 22000 psi, the resulting chitin dispersion is turbid and the diameters of chitin fibers were decreased in comparison to the purified chitin, but those fibers were still largely connected, as shown in Figure 2C,D. The fibrillation of large fibers resulted from mechanical shearing during homogenization.

The obtained purified chitin was dispersed in acidic water resulting in cationization due to the protonation of $-NH_2$ (0.5 wt % of chitin). The cationized chitin dispersion was hazy and had a transmittance of 7% at 800 nm (Figure 3A,D). In contrast, the 0.5 wt % of homogenized chitin dispersion with a pH of 4.1, which was produced by a high pressure homogenization of the cationized chitin, exhibits high transparency and has a transmittance of 81% at 800 nm, as illustrated in Figure 3B,D. Meanwhile, it flowd easily under gravity (Figure 3C) and the homogenized chitin has a zeta potential of +57.5 mV in water at pH 4.1.

After acid treatment, cationized chitin was still present as micron-sized particles, but the fraction of nanofibers with diameters of less than 50 nm increased (Figure 4A,B), which resulted from the fibrillation of fibers with larger diameters. The disintegration of large fibers occurred as a result of mechanical shearing during magnetic stirring aided by electrostatic repulsion between fibers due to protonated $-NH_3^+$ on the chitin surface. As shown in Figure 4C and D, well-dispersed ChNFs were created after high pressure homogenization of the cationized chitin dispersion. These nanofibers have an average diameter (d_{avg}) of 20 nm, mainly ranging from 5 to 50 nm and lengths that vary between hundreds of nanometers to several micrometers. Chitin has very strong intra- and interhydrogen bonding,[6,7] which not only leads to its insolubility in common solvents, but also hinders the defibrillation of large chitin fibers. Previously, Fan et al. prepared individualized ChNFs from squid pen chitin (largely consisting of β-chitin) using a high-power ultrasonication technique, but ChNFs could not be produced from crab α-chitin by this method despite cationization of the chitin under acid conditions (pH 4). It was argued that nonfibrillation of α-chitin may result from its higher crystallinity index, antiparallel configuration and greater intermolecular forces in comparison to β-chitin.[11] The formation of dispersed ChNFs by the high pressure homogenization of crab α-chitin indicates that the strong molecular interactions between chitin can be effectively broken with the combination of the high mechanical shearing induced by the homogenizer and electrostatic repulsion between chitin nanofibers (zeta potential: +57.5 mV at pH 4.1). As shown before, cationized chitin dispersions showed poor transparency while dispersions of homogenized chitin with acidic treatment were transparent. We argue that the different appearances are related to the size of particles in dispersion, since the large chitin particles in the cationized, nonhomogenized dispersion would lead to strong light scattering. It is noteworthy to mention that ChNF dispersions in Figure 3B,C flow easily under gravity, and show high transparency and excellent stability without apparent aggregation over one year. This stability indicates that although the percentage of amino groups in chitin was very low (DA: 92.4%), the positively charged $-NH_3^+$ on ChNFs at pH 4.1 were still quite effective in preventing ChNF aggregation.

The shear viscosities of 0.5 wt % ChNF dispersions were studied as a function of shear rate. As shown in Figure 5, the dispersion in water of pH 4.1 shows shear thinning behavior with increasing shear rate. In addition to ChNF dispersion, the shear thinning of dispersions of chitin nanocrystals and cellulose nanocrystals, microfibers and nanofibers have also been reported previously.[21,25−29] It is understood to be a consequence of breakup of any fiber entanglements as well as fiber orientation in the flow field at higher shear rates. The shear viscosity of ChNFs at 1 rad/s is 0.04 Pa·s, which is close to the reported value of ∼0.01 Pa·s for rodlike cellulose nanowhiskers with similar dimensions at the same concen-

dx.doi.org/10.1021/bm501416q | Biomacromolecules 2014, 15, 4614−4620

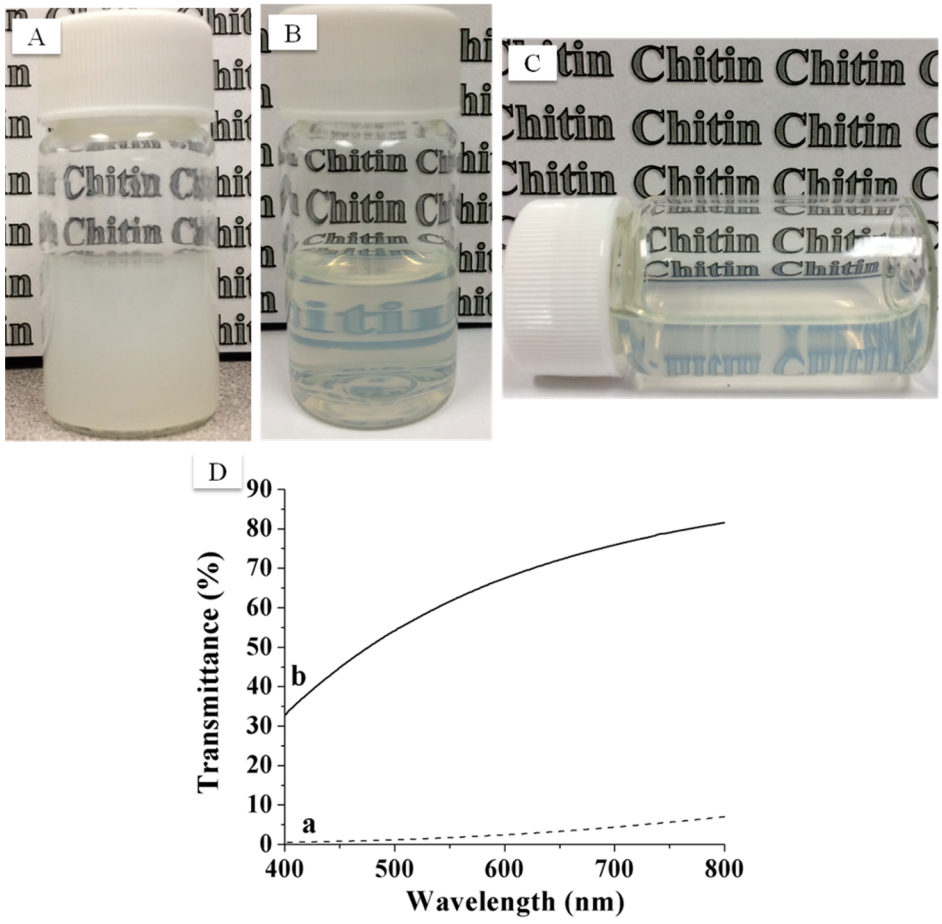

Figure 3. (A) Appearance of cationized chitin dispersion (0.5 wt % of chitin); (B, C) Digital photos of the 0.5 wt % of homogenized chitin in water with pH 4.1, which was produced by a high pressure homogenization process of the cationized chitin/water; (D) Light transmittance spectra of the cationized chitin/water (a) and homogenized chitin/water (pH 4.1, b) in the range of 400−800 nm wavelengths.

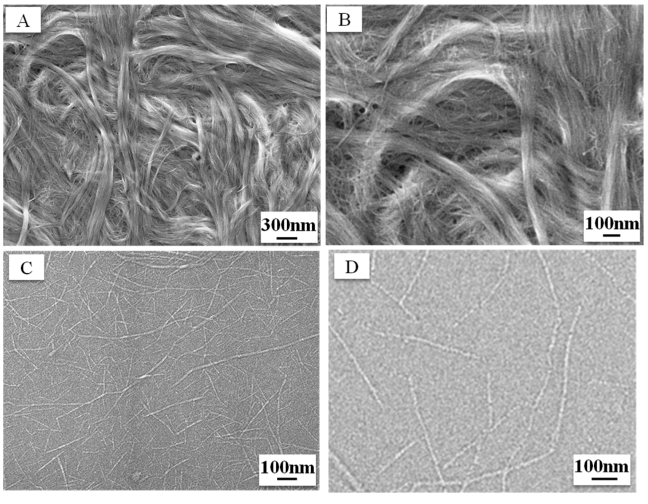

Figure 4. (A, C) SEM images of the cationized chitin and homogenized chitin with a pH of 4.1, respectively; (B, D) SEM images with higher magnification in comparison to (A) and (C), respectively.

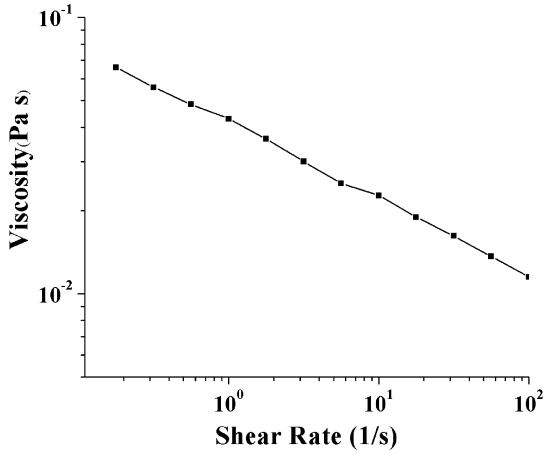

Figure 5. Shear viscosity as a function of shear rate for ChNF/water with a pH of 4.1.

tration of 0.5 wt %.[26] In contrast, highly entangled dispersions of long cellulose nanofibers at the same concentration (0.5 wt %) were reported to have a much large viscosity of ∼1 Pa·s at the same shear rate.[28]

Dynamic rheology results in Figure 6 show that $G' < G''$ over the entire range investigated for the ChNF dispersion, indicating that viscous dissipation dominates mechanical response. In addition to viscosities in Figure 5, this data suggests that the ChNFs did not form strong network structures in water at 0.5 wt %. For example, in the literature for cellulose nanofiber and microfiber dispersions, short, highly charged fibers that do not form strong entanglements generally

dx.doi.org/10.1021/bm501416q | Biomacromolecules 2014, 15, 4614−4620

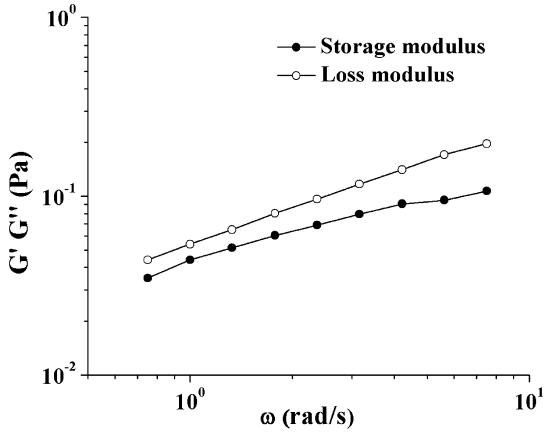

Figure 6. Storage modulus (G') and loss modulus (G'') as a function of frequency for ChNF/water with a pH of 4.1.

show $G' < G''$ at sufficiently low concentration.[25,28] The difference between G'' and G' can be taken as a qualitative indicator of the relative contributions of the viscous and elastic responses. For the ChNF dispersions, G' = 0.044 Pa and G'' = 0.054 Pa for loss modulus at 1 rad/s. Because G' and G'' are of the same order of magnitude and do not differ greatly, there may be weak interactions or entanglements among ChNFs. These values are in a similar range as those reported for negatively charged CNC dispersions with similar dimensions, 10^{-2} to 10^{-1} Pa.[25] However, the reported concentration of CNC dispersions where $G'' > G'$ is lower than 0.5 wt %. In contrast, many reports of CNC dispersions often show $G'' < G'$ even at low concentrations <0.5 wt %, which is nearly always attributed to entanglement and network formation.[25,28,29]

In order to explore the rheological effects of entanglement with longer chitin fibrils, we also prepared partially defibrillated ChNFs by using only four passes through the 0.20 mm nozzle at 15000 psi in the homogenizer. The fibrils in this case are not nearly as well-separated and are larger and longer than the ChNFs discussed above. As shown in Figure 7, the resulting 4-pass chitin/water dispersion has $G' > G''$ and higher storage and loss moduli than the ChNF dispersion produced by 35 passes, indicating the formation of relatively strong networks. For example, G' = 1.7 Pa and G'' = 0.6 Pa at 1 rad/s (Figure 7).

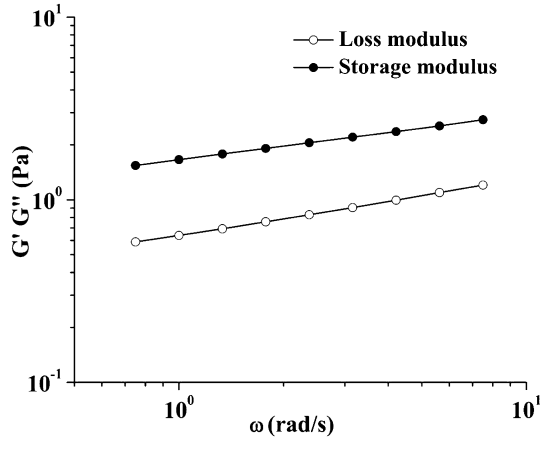

Figure 7. Storage modulus (G') and loss modulus (G'') as a function of frequency for homogenized chitin/water dispersion with a pH of 4.1 after only 4 passes through the 0.20 mm nozzle.

According to Figures 6 and 7, it is apparent that the strong network structures were broken and chitin fibers were shortened with increasing homogenization duration.

When allowed to dry at room temperature, the ChNF dispersion formed an optically transparent and flexible film that is composed of relatively densely packed nanofibers (Figure 8A–C). The mean (Ra) and root-mean-square (rms) surface roughness of the ChNF film were 3.0 ± 0.7 nm and 2.3 ± 0.5 nm, respectively. The film has transmittances of 89% at 800 nm and 80% at 400 nm (Figure 8D) and the high transparency is attributed to low light scattering and adsorption of nanosized ChNFs. The water content of ChNF films was measured by TGA and it was 7.0 ± 0.7%. The film had a density of 1382 kg/m^3 and a porosity of 3% that was calculated according to eq 2. Mechanical tensile testing, for which typical results are shown in Figure 9, indicated that the ChNF film had an ultimate tensile strength of 137 MPa, a Young's modulus of 4.37 GPa, and an elongation at break of 7.4%, which is consistent with previous reports.[10]

Figure 10 shows the normalized ATR-FTIR spectra of the purified chitin powders and ChNF film dried from ChNF dispersion at room temperature. The characteristic peaks of chitin such as amide band I at 1654 and 1620 cm^{-1}, amide band II at 1554 cm^{-1}, OH stretching band at 3478 cm^{-1}, and NH stretching at 3260 and 3098 cm^{-1} are observed from both of these spectra.[4,6,7] In addition, these two spectra do not show any differences in the number of peaks. This indicated that chemical structures of chitin were well maintained after the high pressure homogenization.

All the gas permeabilities of ChNF films were in the range from 0.002 to 0.03 barrer, as shown in Table 1. Owing to its small kinetic diameter, H_2 had the highest gas permeability value in comparison to other gases (CO_2, O_2, N_2, and CH_4).[30] Poly(ethylene terephthalate) (PET), poly(ethylene) (PE), and poly(propylene) (PP) are widely used for packaging applications where O_2 and CO_2 barrier properties are key criteria. PET, PE, and PP have O_2 permeabilities of 0.015–0.076, 0.75–4.73, and 0.75–1.52 barrer, respectively, and CO_2 permeabilities of 0.3, 11.7–14.6, and 4 barrer, respectively.[10,15,31−33] We note that there is variation in gas barrier properties of polymers based on processing and crystallinity, as well as the humidity under which permeability is measured. While we report gas permeabilities under dry conditions here, the behavior of chitin films under humid conditions is the subject of ongoing work. The values provided for comparison to PET, PE, and PP are typical for commercial films under dry conditions. Compared with these synthetic polymer films, the dry O_2 and CO_2 permeabilities of the self-standing pure ChNF films produced here are much lower, only 0.006 and 0.0018 barrer, respectively. This is attributed to the highly crystalline structure of ChNFs, which result in low free volume and low gas permeability.[10,15−17]

To put our results in context, we discuss several recent reports of high barrier property membranes based on cellulose or chitin. Barrier properties that meet or exceed those of commercial barrier polymers such as PET, PVC, and PE were reported for films composed of nanofibrillated cellulose obtained by high-pressure fluidization (flow through a narrow "*z*-shaped" chamber).[18] When concentrated by filtration, a wet gel film was produced which was wet pressed at room temperature and then hot pressed at 100 °C to produce a dense film with an O_2 permeability of 0.00091 barrer (at 23 °C).[18] A remarkably low O_2 permeability for a self-standing cellulose

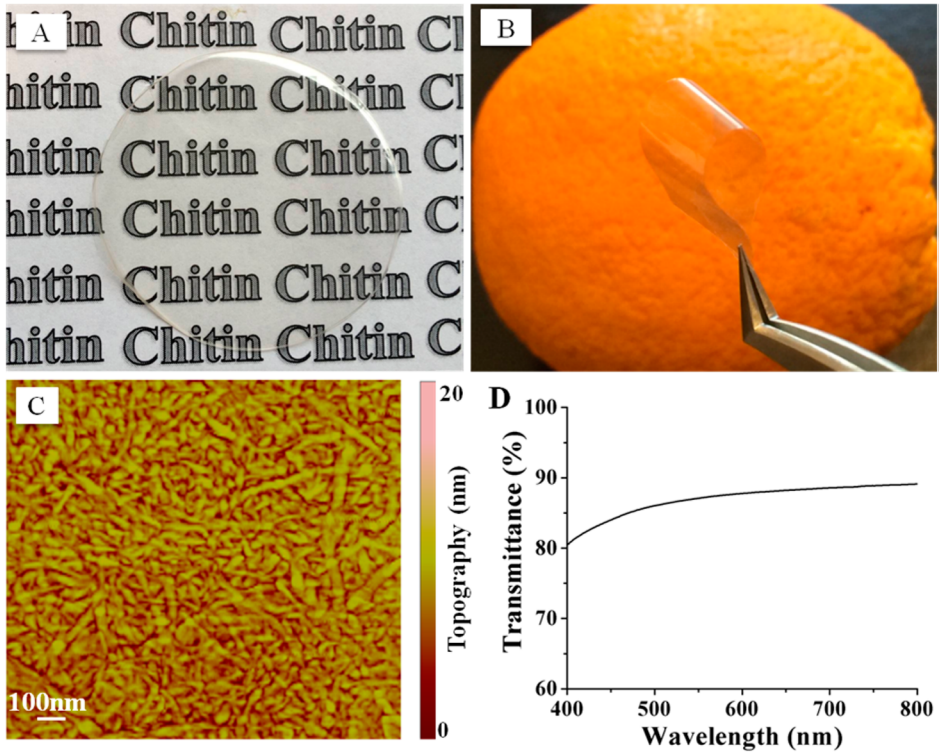

Figure 8. Appearance and flexibility of optically transparent ChNF films: (A) flat film; (B) bent film; (C) AFM topography image obtained from the tapping mode in air at room temperature; and (D) light transmittance spectra of ChNF film in the range of 400 to 800 nm wavelengths.

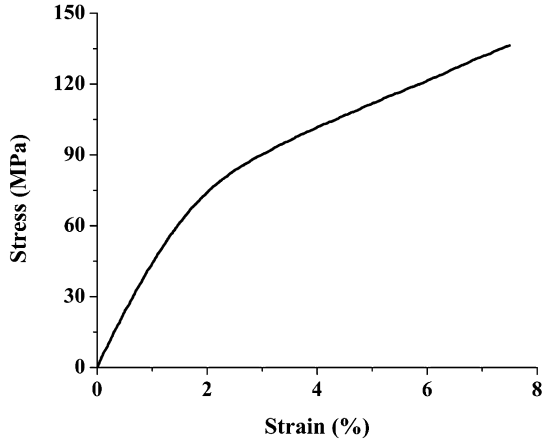

Figure 9. Representative stress−strain curve of the ChNF films.

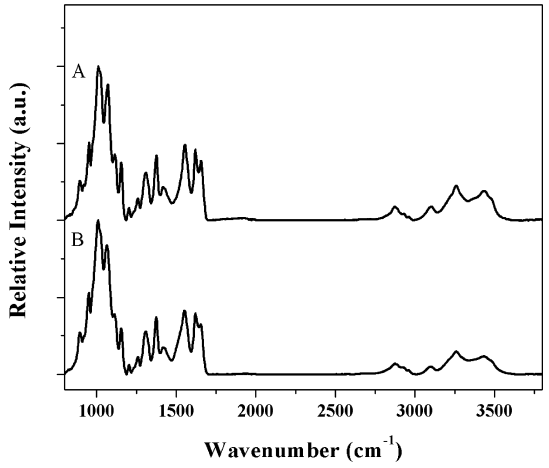

Figure 10. ATR-FTIR spectra of purified chitin powder (A) and ChNF film (B).

membrane was produced by regeneration of cellulose fully dissolved in an NaOH/urea/water solution via a freeze/thawing process.[20] Following addition of acetone coagulant and drying, the resulting film had an O_2 permeability of 4.6×10^{-6} barrer (23 °C), which is lower than the best performing barrier materials commonly used in food packaging, such as poly(vinylidene chloride). When the same freeze/thaw dissolution process was applied to chitin, the chitin was fully dissolved but produced gel films formed after addition of coagulant that were too brittle to survive gas permeation testing. Only after plasticizing with glycerol was a film with O_2 permeability of 0.003 barrer (35 °C) produced.[10] Self-standing films of cellulose nanowhiskers produced by TEMPO oxidation were reported to have O_2 permeability of 7.5×10^{-5} barrer.[19] The chemical TEMPO process was also used to produce chitin nanowhiskers that were dried on PLA films.[21] The composite

Table 1. Gas Permeabilities in ChNF Films at 0% Relative Humidity

gas	kinetic diameter[25] (Å)	permeability (barrer)
H_2	2.89	0.024
CO_2	3.30	0.018
O_2	3.46	0.006
N_2	3.64	0.0034
CH_4	3.80	0.0027

PLA/chitin films had an impressive O2 permeability of 0.001 barrer, lower than PLA itself (0.28 barrer). In the studies referenced here, an inverse correlation between film density and permeability is evident, illustrating the primary importance of preserving fiber crystallinity and alignment or packing nano-

dx.doi.org/10.1021/bm501416q | Biomacromolecules 2014, 15, 4614−4620

fibers during the gelation or drying steps. In the spectra in Figure 8D, the drop-off in transmission at low wavelengths may indicate scattering by small pore defects. Surface topography in the AFM image in Figure 8 may also indicate small surface pores. Density measurements presented above suggest that porosity is near 3%. The good barrier properties indicate that any pores were not highly interconnected. However, this observation suggests that there may be room for improvement in the barrier properties by applying densification strategies to the films to eliminate isolated pores.

CONCLUSIONS

In summary, ChNFs were successfully extracted from crab α-chitin by a high pressure homogenization process under acidic conditions. Neither high pressure homogenization nor cationization of chitin alone could disintegrate large chitin fibers effectively. Rather, only homogenization of cationized chitin was effective in producing ChNFs. The well-fibrillated ChNF had an average diameter of 20 nm and a zeta potential of +57.5 mV at pH 4.1, which arises from protonated $-NH_3^+$ groups that stabilize the dispersion via electrostatic repulsion. The homogenized ChNFs are well dispersed in water without forming strong network structures at room temperature, and the obtained ChNF dispersion has low viscosity and storage modulus. Self-standing, pure chitin films obtained by simply drying the ChNF dispersions exhibited high optical transparency and tensile strength, flexibility, and excellent gas barrier properties. To our knowledge, these are the first reported self-standing, pure chitin films with O_2 and CO_2 barrier properties that exceed PET, an important benchmark for commercial barrier applications. Sustainably sourced nanofibrous materials are potentially useful for applications including food, beverage, electronics, and medicine packaging.

AUTHOR INFORMATION

Corresponding Author

*E-mail: carson.meredith@chbe.gatech.edu.

Notes

The authors declare no competing financial interest.

ACKNOWLEDGMENTS

We are thankful to the Georgia Tech Renewable Bioproducts Institute and the Air Force Office of Scientific Research (Grant # FA9550-10-1-0555) for financial support of this research. Professor Yulin Deng (Georgia Tech) is acknowledged for providing access to the high-pressure homogenizer.

REFERENCES

(1) Serrano-Ruiz, J. C.; Luque, R.; Sepúlveda-Escribano, A. *Chem. Soc. Rev.* **2011**, *40*, 5266−5281.
(2) Irimia-Vladu, M. *Chem. Soc. Rev.* **2014**, *43*, 588−610.
(3) Nair, K. G.; Dufresne, A. *Biomacromolecules* **2003**, *4*, 657−665.
(4) Pillai, C. K. S.; Paul, W.; Sharma, C. P. *Prog. Polym. Sci.* **2009**, *34*, 641−678.
(5) Raabe, D.; Sachs, C.; Romano, P. *Acta Mater.* **2005**, *53*, 4281−4292.
(6) Rinaudo, M. *Prog. Polym. Sci.* **2006**, *31*, 603−632.
(7) Rinaudo, M. *Polym. Int.* **2008**, *57*, 397−430.
(8) Min, B. M.; Lee, S. W.; Lim, J. N.; You, Y.; Lee, T. S.; Kang, P. H.; Park, W. H. *Polymer* **2004**, *45*, 7137−7142.
(9) Zhong, C.; Cooper, A.; Kapetanovic, A.; Fang, Z.; Zhang, M.; Rolandi, M. *Soft Matter* **2010**, *6*, 5298−5301.
(10) Duan, B.; Chang, C.; Ding, B.; Cai, J.; Xu, M.; Feng, S.; Ren, J.; Shi, X.; Dud, Y.; Zhang, L. *J. Mater. Chem. A* **2013**, *1*, 1867−1874.
(11) Fan, Y.; Saito, T.; Isogai, A. *Biomacromolecules* **2008**, *9*, 1919−1923.
(12) Ifuku, S.; Nogi, M.; Abe, K.; Yoshioka, M.; Morimoto, M.; Saimoto, H.; Yano, H. *Biomacromolecules* **2009**, *10*, 1584−1588.
(13) Ifuku, S.; Nogi, M.; Yoshioka, M.; Morimoto, M.; Yano, H.; Saimoto, H. *Carbohydr. Polym.* **2010**, *81*, 134−139.
(14) Wu, J.; Meredith, J. C. *ACS Macro Lett.* **2014**, *3*, 185−190.
(15) Lange, J.; Wyser, Y. *Packag. Technol. Sci.* **2003**, *16*, 149−158.
(16) Lavoine, N.; Desloges, I.; Dufresne, A.; Bras, J. *Carbohydr. Polym.* **2012**, *90*, 735−764.
(17) Miller, K. S.; Krochta, J. M. *Trends Food Sci. Technol.* **1997**, *8*, 228−237.
(18) Österberg, M.; Vartiainen, J.; Lucenius, J.; Hippi, U.; Seppälä, J.; Serimaa, R.; Lai, J. *ACS Appl. Mater. Interfaces* **2013**, *5*, 4640−4647.
(19) Fujisawa, S.; Okita, Y.; Fukuzumi, H.; Saito, T.; Isogai, A. *Carbohydr. Polym.* **2011**, *84*, 579−583.
(20) Yang, Q.; Fukuzumi, H.; Saito, T.; Isogai, A.; Zhang, L. *Biomacromolecules* **2011**, *12*, 2766−2771.
(21) Fan, Y.; Fukuzumi, H.; Saito, T.; Isogai, A. *Int. J. Biol. Macromol.* **2012**, *50*, 69−76.
(22) Duarte, M. L.; Ferreira, M. C.; Marvão, M. R.; Rocha, J. *Int. J. Biol. Macromol.* **2001**, *28*, 359−363.
(23) Kasaai, M. R. *Carbohydr. Polym.* **2010**, *79*, 801−810.
(24) Rungta, M. Carbon Molecular Sieve Dense Film Membranes for Ethylene/Ethane Separations. *Ph.D. Dissertation*, Georgia Institute of Technology, Atlanta, GA, November, 2012.
(25) Benhamoua, K.; Dufresne, A.; Magninc, A.; Mortha, G.; Kaddami, H. *Carbohydr. Polym.* **2014**, *99*, 74−83.
(26) Lima, M. M. S.; Borsali, R. *Macromol. Rapid Commun.* **2004**, *25*, 771−787.
(27) Orts, W. J.; Godbout, L.; Marchessault, R. H.; Revol, J. F. *Macromolecules* **1998**, *31*, 5717−5725.
(28) Pääkkö, M.; Ankerfors, M.; Kosonen, H.; Nykänen, A.; Ahola, S.; Österberg, M.; Ruokolainen, J.; Laine, J.; Larsson, P. T.; Ikkala, O.; Lindström, T. *Biomacromolecules* **2007**, *8*, 1934−1941.
(29) Tatsumi, D.; Ishioka, S.; Matsumoto, T. *J. Soc. Rheol., Jpn.* **2002**, *30*, 27−32.
(30) Low, B. T.; Chung, T. S.; Chen, H.; Jean, Y.; Pramoda, K. P. *Macromolecules* **2009**, *42*, 7042−7054.
(31) Gholizadeh, M.; Razavi, J.; Mousavi, S. A. *Mater. Des.* **2007**, *28*, 2528−2532.
(32) Jarus, D.; Hiltner, A.; Baer, E. *Polymer* **2002**, *43*, 2401−2408.
(33) Tsai, T.; Li, C.; Chang, C.; Cheng, W.; Hwang, C.; Wu, R. *Adv. Mater.* **2005**, *17*, 1769−1773.